VISSR ATMOSPHERIC SOUNDER

Monthly Progress Report No. 7
For the Period 1 Mar. 1974 to 31 Mar. 1974

Contract No. NAS5-21965

For National Aeronautics and Space Administration
Goddard Space Flight Center
Glen Dale Road
Greenbelt, Maryland 20771

by

V. E. Suomi, Principal Investigator
L. A. Sromovsky, Co-Investigator

The University of Wisconsin
Space Science and Engineering Center
1225 West Dayton Street
Madison, Wisconsin 53706

TABLE OF CONTENTS

I. Introduction

In addition to continued simulation studies, which are still not in reportable form yet, work on aspects of system performance, radiative and electronics calibration of the VISSR, and ground processing approaches have yielded reportable results. Full details of most of these results have already been communicated to NASA in other documents.

II. System Performance Studies

1. The Meaning of Absolute and Relative Errors

Suppose radiance measurements are made in two spectral bands ν_1 and ν_2 of scene radiances N_1 and N_2 with equivalent blackbody temperatures T_1 and T_2 such that

$$N_1 = c_1\nu_1^3[e^{c_2\nu_1/T_1} - 1]^{-1}, \text{ and}$$

$$N_2 = c_1\nu_2^3[e^{c_2\nu_2/T_2} - 1]^{-1}.$$

In $\tilde{N}_1$ and $\tilde{N}_2$ are measured radiances and $\tilde{T}_1$ and $\tilde{T}_2$ are equivalent blackbody temperatures derived from these radiances using the inverse Planck function

$$\tilde{T}_{1,2} = c_2\nu_{1,2}[\ln(c_1\nu_{1,2}^3/\tilde{N}_{1,2} + 1)]^{-1}$$

then the absolute errors of these spectral bands may be expressed in terms of either temperature or radiance as

$$(\Delta N_1)_A = \tilde{N}_1 - N_1, \ (\Delta N_2)A = \tilde{N}_2 - N_2 \text{ and}$$

$$(\Delta T_1)_A = \tilde{T}_1 - T_1, \ (\Delta T_2)_A = \tilde{T}_2 - T_2.$$

In general both absolute temperature and radiance errors can vary with signal and wavelength. However, there is good reason to choose the

temperature representation since it has the most direct bearing on the ultimate object of the measurements, i.e. atmospheric temperature profiles, and thus required accuracy in this representation will show the smallest variation with wavelength.

Relative errors between bands ν_1 and ν_2 are simply the differences in absolute errors, i.e.

$$(\Delta N_{1,2})_R = (\Delta N_1)_A - (\Delta N_2)_A, \text{ and}$$

$$(\Delta T_{1,2})_R = (\Delta T_1)_A - (\Delta T_2)_A.$$

It should be noted that the statement of a requirement on relative radiance error between 3.7 μ and 11.2 μ spectral bands is not at all appropriate since a tolerable absolute error of 1.0 mW/(cm^2-cm^{-1}-ster) for the 11.2 μ band is, in many cases, larger than the signal level for the 3.7 μ band. For reference, for the 15 μ CO_2 band spectral bands the requirement of 1.0 mW/(cm^2-ster-cm^{-1}) absolute radiance error and 0.25 mW/(cm^2-ster-cm^{-1}) relative error leads to the following absolute and relative temperature errors:

$$(\Delta T)_A \simeq 1.5° \text{ peak; and} \quad (\Delta T_{1,2})_R \simeq 0.5° \text{ peak.}$$

The peak absolute error occurs when equivalent scene temperatures are very low ($\simeq$ 200°K), and the peak relative error occurs between spectral bands viewing very different equivalent scene temperatures ($\simeq$ 200°K for one, and $\simeq$ 300°K for the other).

2. Effects of Calibrator Temperature Errors

In order to calibrate the VAS radiometer output it is necessary to determine an equivalent blackbody temperature (or radiance) which, if placed outside the VAS telescope, would produce the same response as shutter insertion. The exact value of this equivalent temperature will be

denoted by T_s and the estimated value $\tilde{T}_s$. Additional notation required is defined below:

T_t, $\tilde{T}_t$ = exact and measured values of equivalent blackbody scene temperatures

N_ν, $\tilde{N}_\nu$ = exact and measured values of scene radiances.

The calibration equation scales the observed output while viewing the scene to the output obtained from the calibration shutter so that the measured scene radiance is given by

$$\tilde{N}_\nu(T_t) = N_\nu(T_t) \frac{N_\nu(\tilde{T}_s)}{N_\nu(T_s)} .$$

Since, for $e^{c_2\nu/T} \gg 1$ and $|\tilde{T}_s - T_s| \ll T_s$,

$$\frac{N_\nu(\tilde{T}_s)}{N_\nu(T_s)} \simeq e^{c_2\nu(\frac{1}{T_s} - \frac{1}{\tilde{T}_s})},$$

and similarly for $N(T_t)$ and $N(T_t)$ we can approximate T_t by the expression

$$\tilde{T}_t = T_t + (\tilde{T}_s - T_s) \frac{T_t^2}{T_s^2},$$

which shows that the absolute equivalent temperature error of a measured radiance due to temperature errors in T_s is, to good approximation, independent wavelength and strongly dependent on scene temperature, i.e.

$$(\tilde{T}_t - T_t) = (\tilde{T}_s - T_s) \frac{T_t^2}{T_s^2} .$$

Thus the relative temperature error between channels depends only on the equivalent scene temperatures. If we define,

$$(\Delta T_t)_A = \tilde{T}_t - T_t$$

$$(\Delta T_s)_A = \tilde{T}_s - T_s,$$

then the relative error between two spectral bands is given by

$$(\Delta T_{1,2})_R = (\Delta T_{1,t})_A - (\Delta T_{2,t})_A = (\Delta T_s)_A \left[\frac{T_{1,t}^2 - T_{2,t}^2}{T_s^2}\right].$$

Table 1 displays two extreme cases of relative and absolute temperature errors due to an error in T_s of 0.57°K. The worst case occurs for a tropical atmosphere which displays a large temperature range. In this case the peak to peak error is $\simeq 1/2\Delta T_s$. The best case is for an arctic atmosphere which has a relatively small range of temperatures. In the latter case the peak to peak relative error is $\simeq 1/10\Delta T_s$. In both cases the absolute error is less than 1.5°K and the relative error is less than 0.5°K.

3. Radiance Errors Including Noise

Using N to denote the measured (and erroneous) value of N and the notation of section IV, the measured and exact radiances are given by the linearization equations for the kth spectral band:

$$\tilde{N}_t^k = \tilde{N}_{SH}^k \frac{\tilde{S}(\tilde{DN}_t^k) - \tilde{S}(\tilde{DN}_{sp}^k)}{\tilde{S}(\tilde{DN}_{SH}^k) - \tilde{S}(\tilde{DN}_{sp}^k)},$$

$$N_t^k = N_{SH}^k \frac{S(DN_t^k) - S(DN_{sp}^k)}{S(DN_{SH}^k) - S(DN_{sp}^k)}.$$

The error in obtaining a sample number appropriate to a radiance N is a result of two errors: (1) uncertainty in the digital level corresponding to N; and (2) uncertainty in the transfer function between sample number and digital number. The first error is denoted by ΔDN and the second by ΔS. The combined error is thus

$$\tilde{S}(\tilde{DN}) - S(DN) = \Delta S + \frac{\partial S}{\partial DN}.\Delta DN$$

Table 1. Relative and Absolute Temperature Errors Resulting from $\Delta T_s = 0.57°K$

$\nu(cm^{-1})$	ARCTIC ATMOSPHERE			TROPICAL ATMOSPHERE		
	Brightness TEMP (°K)	ABS ΔT	REL $\Delta T - \overline{\Delta T}$	Brightness TEMP (°K)	ABS T	REL $\Delta T - \overline{\Delta T}$
680	228	.33	-.03	227	.33	-.10
692	228	.33	-.03	217	.30	-.13
703	229	.33	-.03	232	.34	-.09
715	235	.35	-.01	252	.40	-.03
745	244	.38	+.02	274	.48	+.05
760	246	.38	+.02	282	.50	+.08
*790	245	.38	+.02	278	.49	+.06
895	249	.39	+.03	296	.56	+.13
*2335	235	.35	-.01	231	.34	-.09
*2680	249	.39	+.03	296	.56	+.13

* These are estimated values.

The difference between $\tilde{N}_t^k$ and N_t^k is thus found to be

$$\Delta N_t^k = \Delta N_{SH}^k \cdot \frac{S_t^k - S_{sp}}{S_{SH}^k - S_{sp}} + \Delta S_t^k \frac{N_{SH}}{S_{SH}^k - S_{sp}^k} - \Delta S_{SH}^k \frac{N_{SH}^k (S_t^k - S_{sp}^k)}{(S_{SH}^k - S_{sp}^k)^2}$$

$$+ \Delta S_{sp}^k N_{SH}^k \frac{S_t^k - S_{SH}^k}{(S_{SH}^k - S_{sp}^k)^2} + \Delta DN_t^k \cdot \frac{\partial S}{\partial DN} \cdot N_{SH}^k \frac{1}{(S_{SH}^k - S_{sp}^k)}$$

$$- \Delta DN_{SH}^k \cdot \frac{\partial S}{\partial DN} \cdot N_{SH}^k \frac{S_t^k - S_{sp}^k}{(S_{SH}^k - S_{sp}^k)^2} + \Delta DN_{sp}^k \cdot \frac{\partial S}{\partial DN} \cdot N_{SH}^k \frac{S_t^k - S_{SH}^k}{(S_{SH}^k - S_{sp}^k)^2}$$

where we have used the notational form $S(DN_{SH}^k) = S_{SH}^k$, etc. Since exact sample values are linear with exact radiance, by expressing all parameters as radiance equivalents it is possible to reduce the above expression to the simpler form

$$\Delta N_t^k = \beta_t \Delta N_{SH}^k + (\Delta S_t^k + \Delta DN_t^k) - \beta_t (\Delta S_{SH}^k + \Delta DN_{SH}^k) - (1 - \beta_t) \cdot$$

$$\cdot (\Delta S_{sp}^k + \Delta DN_{sp}^k)$$

where $\beta_t = \frac{N_t^k}{N_{SH}^k}$.

III. Calibration Analysis

The VAS uses a two point calibration system. The radiance references are space ($\tilde{}$ zero radiance) and an internal blackbody. However, since the internal blackbody does not calibrate the primary optical system the accuracy of the calibration depends on measurements of temperatures of primary optical components and on estimation of their effective radiances. A model of the effects of the primary optics on the calibration accuracy is developed in the following section.

1. Model for Primary Optics Emission

Refer to Figure 1 for identification of the optical components whose parameters are defined below.

Definitions:

$\varepsilon_1, \varepsilon_2, \varepsilon_3$ = emissivities of mirrors 1, 2, 3.

$R_{s,1}, R_{s,2}, R_{s,3}$ = specular reflectivities of mirrors 1, 2, 3.

$R_{d,1}, R_{d,2}, R_{d,3}$ = diffuse reflectivities of mirrors 1, 2, 3.

ε_o = emissivity of central obscuration

R_o = combined diffuse and specular reflectivity of central obscuration

ε_f = emissivity of field lens

R_f = total reflectivity of field lens

τ_f = transmission of field lens

K = obscuration fraction

T_1, T_2, T_3 = temperatures of mirrors 1, 2, 3.

T_o = temperature of central obscuration

T_f = temperature of field lens

T_E = temperature of an external blackbody

T_s = temperature of internal blackbody calibrator

$T_{A,i}$ = effective average temperature of radiation diffusely scattered by the ith mirror into the optical beam.

$T_{A,0}$ = effective average temperature of radiation scattered by the central obscuration into the optical beam.

$T_{A,f}$ = effective average temperature of radiation reflected by the field lens into the optical train.

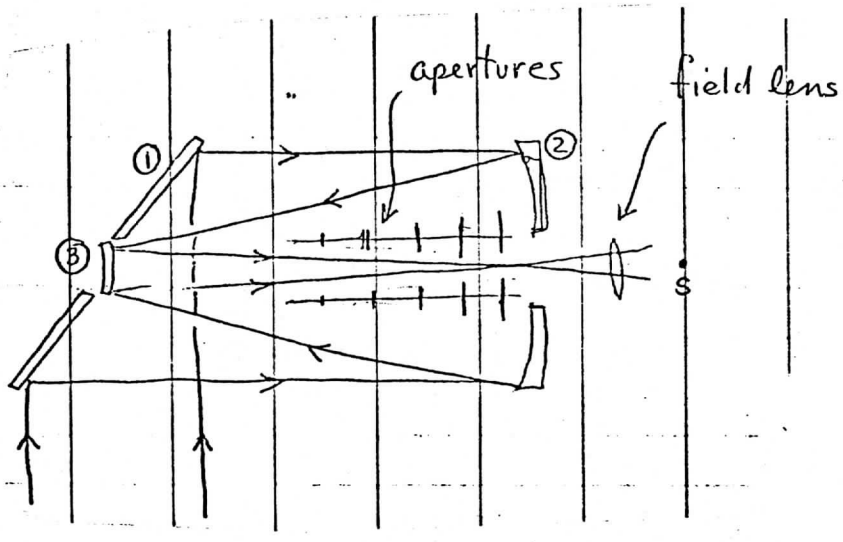

Figure 1. Schematic of primary optical components and field lens. The internal calibration blackbody is introduced at point 5.

Identities:

$$\varepsilon_i + R_{s,i} + R_{d,i} = 1 \qquad \text{for } i = 1, 2, 3$$

$$\varepsilon_f + \tau_f + R_f = 1$$

$$\varepsilon_o + R_o = 1$$

2. Estimation of the VAS Response to an External Blackbody

At a point (s) downstream from the field lens the apparent radiance of an external blackbody is the sum of the attenuated emission from the source and the emission from the primary optics. The general expression for this radiance is given below:

$$N_{Eff} = B(T_E)R_{s,1}R_{s,2}R_{s,3}\,\tau_f(1-K)$$

$$+ \tau_f(1-K)\{R_{s,2}R_{s,3}[B(T_{A,1})R_{d,1} + B(T_1)\varepsilon_1] + R_{s,3}[B(T_{A,2})R_{d,2} + B(T_2)\varepsilon_2]\}$$

$$+ \tau_f K\, R_{s,3}\{B(T_{A,o})R_o + B(T_o)\varepsilon_o\} + \tau_f\{B(T_{A,3})R_{d,3} + B(T_3)\varepsilon_3\}$$

$$+ \{B(T_{A,f})R_f + B(T_f)\varepsilon_f\}$$

If all optical components are at a temperature equal to the external source, the radiance at s should be just $B(T_E)$.

3. Special Case Model of Radiometric Calibration Uncertainty

The VAS blackbody is inserted at s with temperature T_s. In order to calibrate the VAS it is necessary to determine the externally applied radiance which produces the same response, i.e., T_E must be found such that $N_{Eff} = B(T_s)$ even when the VAS is not isothermal with the shutter.

In order to obtain an approximate estimate of the uncertainty in determining T_E for a given T_s, it will be assumed that all optical component temperatures are the same except for the internal blackbody temperature, i.e., $T_1 = T_{A,1} = T_2 = T_{A,2} = T_3 = T_{A,3} = T_0 = T_{A,0} = T_f = T_{A,f} = T_A$.

Under these assumptions the requirement is

$$B(T_E)R_{s,1}R_{s,2}R_{s,3}\,\tau_f(1-K) + B(T_A)\,\{1 - \tau_f(1-KR_{s,1}R_{s,2}R_{s,3}\} = B(T_s).$$

If we expand B(T) about T_s then

$$B(T) = B(T_s) + (\frac{\partial B}{\partial T})_{T_s}\,(T-T_s) + \ldots$$

Keeping only terms up to first order in $(T-T_s)$ we can further simplify the requirement to the form

$$(T_E-T_s)R_{s,1}R_{s,2}R_{s,3}\,f(1-K) + (T_A-T_s)\,\{1-\tau_f(1-K)R_{s,1}R_{s,2}R_{s,3}\} = 0.$$

Solving for T_E we obtain

$$T_E = T_s + (T_s-T_A)\,[\frac{1}{R_{s,1}R_{s,2}R_{s,3}\tau_f(1-K)} - 1].$$

This is in disagreement with SBRC's result which has the same form except for the replacement of $1 - \varepsilon_i$ for $R_{s,i}$. Since

$$1 - \varepsilon_i = R_{s,i} + R_{d,i},$$

agreement is obtained if $R_{d,i} \simeq 0$. Even for $R_{d,i} \neq 0$, the disagreement is small since $R_{d,i} << R_{s,i}$. Given the gross approximations made to obtain the above result, the disagreement is certainly a trivial one.

For nominal values of

$$R_{s,1} = R_{s,2} = R_{s,3} = .96$$

$$\tau_f = .90$$

$$K = .16$$

we have $R_{s,1}R_{s,2}R_{s,3}\tau_f(1-K) = .885 \times .9 \times .84 = 0.680.$

and $T_E = T_s + (T_s-T_A) \times (0.471)$

Using SBRC uncertainties of

$\Delta T_s = 0.24°K$

$\Delta(0.471) = 0.163$

$\Delta T_A = .82°K$

and for an assumed difference $T_s - T_A \simeq 2°K$, the RSS error in T_E is $\Delta T_E = 0.57°K$. (The value for ΔT_A is implicit).

IV. Ground Processing Procedures

1. Calibration and Linearization

Radiometric output from the VAS infrared channels is digitally encoded in an 8-bit format (levels 0-255) by an imperfect A/D converter. In order to interpret these somewhat non-linear digital levels in terms of radiance, it is necessary to use a correction algorithm which simultaneously incorporates calibration and linearization. The electronics calibrate ramp, indicated in Figure 2, inserts a voltage at the analog input which is linearly increasing in time. This results in a digital output which stays at a fixed level for a short time period (approximately 68 μsec, or 8.6 samples), then switches to the next highest level, and so on. The relative sample number (which is linear in the voltage and radiance) at which digital levels change is used to linearize the digital area.

The following definitions are required:

$S(DN)$ = Relative sample number corresponding to a digital level DN. (For integral values of DN, S is taken as the midpoint between transitions from and to the level DN; for fractional values of DN, linear interpolation between integral values is used to obtain S).

N_{SH}^k = The effective blackbody radiance in band k of the blackbody outside the VISSR which would give the same response as the internal blackbody. (How this is determined from the blackbody temperature, and other component temperatures is discussed in section III).

N_t^k = The radiance of the scene (target) in spectral band k.

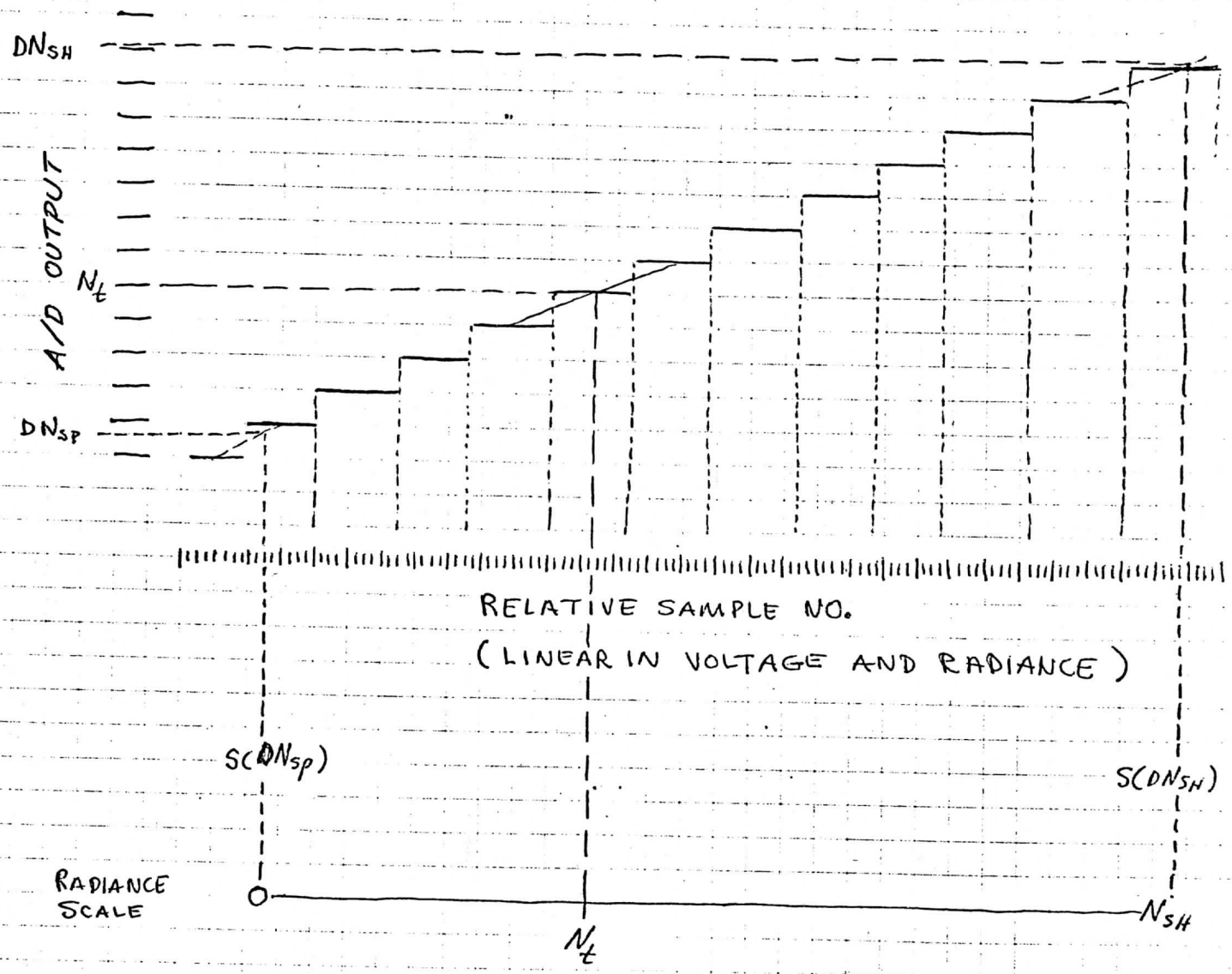

Figure 2. Linearization of A/D Output using Electronics Calibrate Linear Voltage Ramp

DN_t^k = Digital level observed for scene radiance N_t^k. (For a single sample DN_t^k is an integral value).

DN_{sp}^k = The digital output corresponding to the zero offset voltage for band k (the average output while viewing space). This is a fractional number determined during the calibration sequence.

DN_{SH}^k = The digital level (non-integral) corresponding to the radiance N_{SH}^k. This is obtained at the beginning of each line and applies to the previous line.

The expression for N_t^k is then: $$N_t^k = \frac{S(DN_t^k) - S(DN_{sp}^k)}{S(DN_{SH}^k) - S(DN_{sp}^k)} \cdot N_{SH}^k$$

where S(DN) is derived from calibration of a low gain channel and assumed constant for all other bands, i.e. the VAS amplifiers are assumed linear.

2. Possible Approaches to Clear Column Radiance Retrieval and Profile Derivation

Within the area covered by a dwell sounding swath, a target area of approximately 150 km x 150 km is selected for sounding. An area this size contains approximately 550 samples for 0.384 mr FOV's and 1100 samples for 0.192 mr FOV's. In order to derive soundings by inverting the radiative transfer equation, it is first desirable to obtain from this large set of samples best estimates for equivalent clear column radiances in each spectral band. Some of the samples will be unambiguously clear and will receive the greatest weight; the remainder will have varying degrees of cloud contamination and will be corrected by means of projection techniques and weighted according to the estimated error of the projection. The weighted average that results will be used as clear column radiances for the whole grid.

There are many procedures which can be used to make the determinations just discussed. Some of them may be more or less suited to the pecularities of the VAS data, although it is not possible at this time to make a final

choice. Those presently under consideration at Wisconsin are briefly described in the following list of data processing stages.

(1) Derive clear column window channel radiances appropriate to the area for which a sounding is to be made

METHODS (1.1) Histogram analysis of 11.2μ, 0.192 mr samples

(1.2) Histogram analysis of 11.2μ, 0.4 mr samples

(1.3) Histogram analysis of 3.7 μ, 0.4 mr samples

(1.4) Selection of clear fields based on agreement between 3.7 μ and 11.2 μ equivalent blackbody temperatures

(1.5) Projection techniques based on pairs of 3.7 μ and 11.2 μ samples defining a line which intersects the blackbody emission curve at two points, the upper (high radiance) point corresponding to surface emission, the lower to cloud emission.

(2) Find clear column sounding channel radiances appropriate to the area for which a sounding is to be obtained.

METHODS (2.1) Projection techniques based on 11.2 μ window (0.4 mr) and sounding channel radiance plots. Data pairs for the entire area would be plotted, cloud lines identified, and projections made for the flattest line.

(2.2) Paired FOV projection, in which $N^* = N_1/N_2$ is determined for each FOV pair from 11.2 μ (0.4 mr) radiances; a check of each pair is made with 11.2 μ (0.192 mr) and 3.7 μ (0.384 mr) bands, and if agreement is obtained a clear column projection is made for each pair; weighted averages of the projected values yield best estimates for the entire area to be sounded.

(3) Derive temperature profiles from clear column radiances

METHODS (3.1) Regression solution (relies on correlation matrices between temperature deviation measured from the surface and radiances observed from the satellite, derived from large set of comparisons and varies with latitude and season).

(3.2) Matrix inversion - statistical method (depends on a prior statistics of atmospheric temperature profile variance in the form of two covariance matrices).

(3.3) Matrix inversion - "minimum information" solution (simplifying assumption reduces the covariance matrices of (3.2) to being proportional to the identity matrix).

(3.4) Iterative methods - explicitly non-linear.

3. Effects of Registration Errors

In many of the techniques discussed in the previous section, decisions are based on radiances in several spectral bands for the same FOV. However, there are many sources of error which make it difficult to precisely register FOV's in different bands. These registration errors can be divided into two groups:

(1) Errors affecting registration of FOV's of different bands using different detectors

(1.1) Responsivity variations across the detector surface (see Figure 3)

(1.2) Size and position errors in detector array fabrication (see Table 2)

(1.3) Blur variations with field angle (see Figure 4)

(1.4) All the errors listed in the second group.

(2) Errors affecting registration of FOV's of different bands using the same detector

(2.1) Location errors due to discontinuous sampling (since sampling phase is random from spin to spin, this error can be reduced by averaging repeated scans of the same line; the RMS value for a single sample is 24 μ radians, for a 16 spin average it drops to 6 μ radians).

(2.2) Diffraction variations with wavelength (see Figure 5 and Table 3).

It is obvious from the above that registration of different spectral bands is much easier if they use the same detector, the only significant error in that case being diffraction variations with wavelength. This has significance in the selection of data processing procedures from those considered in the previous section. It is useful to group those procedures

into two groups also, one group affected only by group (2) registration errors and the other affected by group (1) and group (2) errors.

(1) Data Processing algorithms that require registration of FOV's using the same detector: (1.1), (1.2), (1.3)
(2.1)

(2) Data processing algorithms that require registration of FOV's of different detectors: (1.4), (1.5)
(2.2)

Thus, the most significant registration problem is that of correcting the registration errors between 3.7 μ and 11.2 μ bands, since these are very useful for checking paired FOV's for cloud type differences. There is an algorithm for correcting this error on a statistical basis, but its effect on clear column retrievals has not yet been verified.

Table 1. Geometrical Errors in Detector Array Fabrication

ITEM	EQUIVALENT ANGULAR ERROR
Centroid Position Error on a Substrate	± 3μr (InSb) ± 7μr (HgCdTe)
North-South Alignment of InSb Array Relative to HgCdTe Array	± 30μr (without correction) ± 15μr (with cooler rotation)
Detector Size Error	± 14μr (in linear dimensions)

Table 3. Wavelength Dependence of Detector Effective IFOV

Wavelength	Fraction of total response originating from within a circle of indicated radius (mr)				
	50%	80%	90%	99%	99.9%
3.73	.138	.175	.187	.310	3.10
6.71	.140	.179	.195	.561	5.61
11.17	.143	.187	.219	.928	9.28
14.71	.146	.195	.240	1.222	12.22
11.17a	.076	.107	.148	.928	9.28

a .192 mr detector. All other wavelengths are for a .384 mr detector.

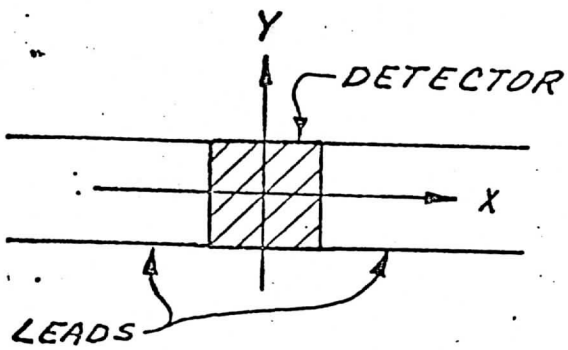

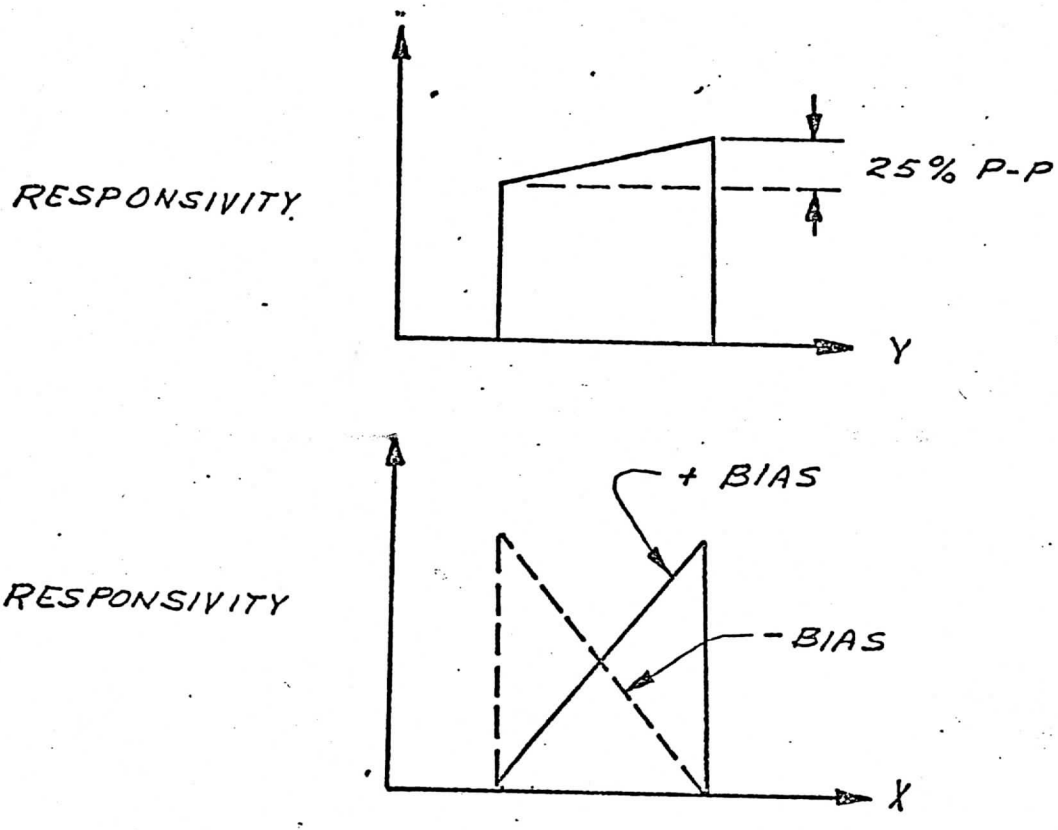

Figure 1. HgCdTe Detector Responsivity Variations

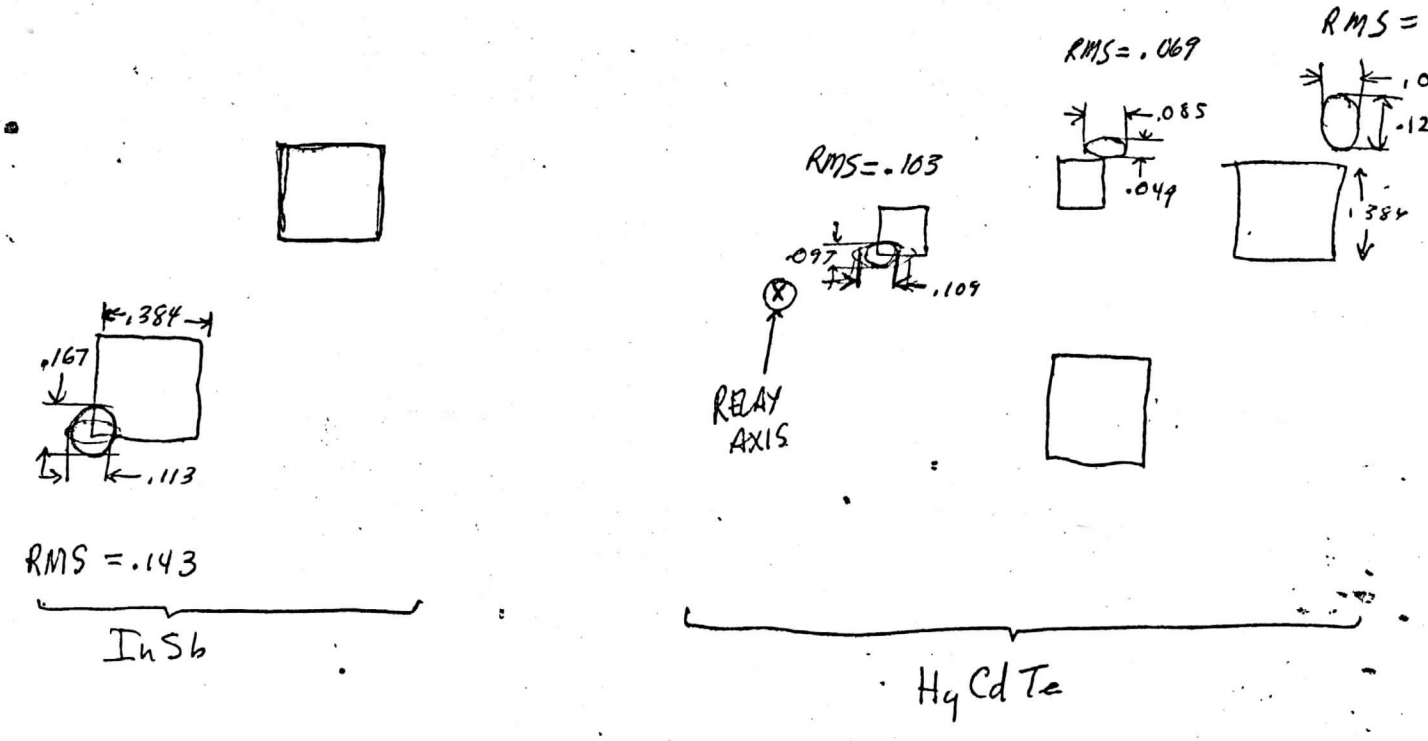

Figure 4. Blur Variations with Field Angle

Fraction of total response originating outside of a circle of Radius R.

R: Radius (mr)

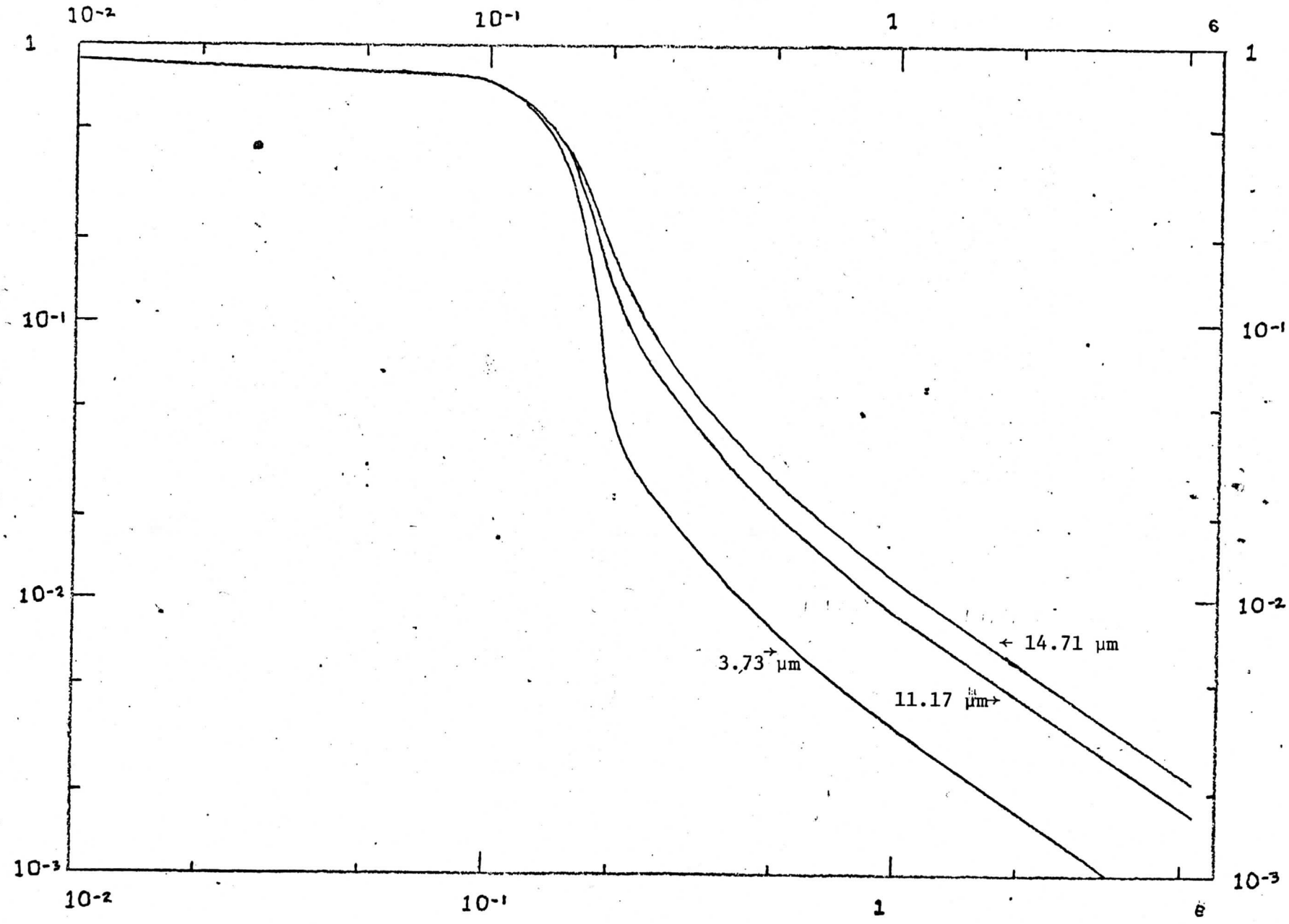

Figure 5. Effects of Diffraction on the Detector Field of View